

# COMPUTATION OF NEUTRON CROSS SECTIONS FROM 15 MeV TO 200 MeV FOR $A \geq 40$

**Robert E. Shamu** and Stephen M. Ferguson  
*Department of Physics, Western Michigan University  
Kalamazoo, MI 49008*

Randy L. Schutt  
*2134 Perry Street  
Holland, MI 49423*

Knowledge of the symmetry potential of the phenomenological optical model is essential for computing nucleon-nucleus cross sections over a wide range of  $A$ . In the present study we evaluate the symmetry dependence of the real and imaginary parts of the central phenomenological optical potential for neutron-nucleus scattering. We proceed as follows. First, we analyze  $n - {}^{208}\text{Pb}$  differential cross sections for elastic scattering  $\sigma(\theta)$  from 13.5 to 65 MeV [1-4] and  $n - {}^{208}\text{Pb}$  total cross sections  $\sigma_t$  up to 200 MeV [5] to determine optical model parameters for neutrons on  ${}^{208}\text{Pb}$ . Second, we use the results of these neutron analyses along with results for protons on  ${}^{208}\text{Pb}$  [6] to obtain the real, surface imaginary, and volume imaginary Lane potentials for neutrons over the energy range 15 to 65 MeV, for which range compound nucleus and nuclear structure effects (see, e.g., [7]) are believed to be negligible, and for which the energy dependence of the potential strengths for protons [6] and for neutrons [8] appear to be linear. Third, we test the validity of these Lane potentials over the neutron energy range 15 - 65 MeV by comparing computed  $\sigma_t$  with recently measured values [9] for the spherical nuclei  ${}^{40}\text{Ca}$  and  ${}^{90}\text{Zr}$ .

Neutron -  ${}^{208}\text{Pb}$  data were analyzed using the optical model code SNOOPY8 [10]. This code utilizes relativistic kinematics. In accord with the proton work [6], a Woods-Saxon form factor or its derivative was assumed for the radial dependence of each potential. Except for the real diffuseness parameter  $a_0$ , which was fixed at 0.697 fm, parameters utilized for the central potential geometry and spin-orbit potential were average proton values [6].

Differential cross sections for the elastic scattering of neutrons from  ${}^{208}\text{Pb}$  were analyzed at 13.5 MeV [1], 20 MeV and 22 MeV [2], 30.3 MeV and 40 MeV [3], and 65 MeV [4]. At each energy searches were conducted for the potential depths  $V$ ,  $W_D$  and  $W_V$ . Good visual fits were

obtained at each energy and the reduced chi squared,  $\chi_r^2$ , ranged from 3.4 at 65 MeV to 15.5 at 20 MeV and averaged about 8. Additional searches were performed at 13.5 MeV and 65 MeV with  $W_V = 0$  and  $W_D = 0$ , respectively. In both cases neither  $\chi_r^2$  nor the remaining two parameters changed significantly. Results from these searches are plotted in figures 1 and 2 as solid squares. Since  $W_D$  is known to change slope near 14 MeV [11], only values of  $W_D$  from searches for  $E > 14$  MeV are plotted.

It is well known that the sum of imaginary potential strengths  $W = W_D + W_V$  is determined more accurately than either parameter alone. For the neutron strengths in figure 2, the intercept between  $W(E)$  over the energy range  $20 \text{ MeV} \leq E \leq 40 \text{ MeV}$  and  $W_D(E)$  for  $E < 14 \text{ MeV}$  (see [7]) is at  $(13.9 \pm 1.1) \text{ MeV}$ , i.e., at this energy  $W_V \equiv 0$  and  $W_D$  changes slope. In figure 2 the solid squares at 14 MeV are included to take these two constraints into account. Here the solid lines are fits to the solid squares which are required to pass through the 14-MeV points. For  $W_V$ , only the energy range for which the energy dependence of  $W(E)$  appeared to be linear,  $E \leq 40 \text{ MeV}$ , was fitted.

It is apparent from figure 2 that  $W_V(E)$  for neutrons cannot be represented by a linear function over the entire energy range  $14 \text{ MeV} \leq E \leq 65 \text{ MeV}$ . In agreement with [5], we find from fitting  $\sigma_t$  that a quadratic function for  $W_V(E)$  is satisfactory.

At higher energies, where at present neutron data are predominately total cross sections,  $V(E)$  and  $W_V(E)$  were determined by necessity from fitting the energy and magnitude, respectively, of the  $^{208}\text{Pb}$   $\sigma_t$  maximum near 80 MeV (see figure 3). The function  $V(E)$  was assumed to be logarithmic for  $E \geq 60 \text{ MeV}$ , in accord with previous neutron [5] and proton [6,10] analyses; and  $W_V(E)$  was assumed to be linear, an energy dependence which proved to be satisfactory over a wide energy range. Because of continuity requirements, a total of only three parameters could be adjusted to fit these high-energy  $\sigma_t$ . For  $V(E)$ , both the value and slope at 58 MeV were required to be continuous; for  $W_V(E)$ , only the value at 63 MeV was required to be continuous. Our fit to  $^{208}\text{Pb}$   $\sigma_t$  data [5] over the energy range 14 MeV to 200 MeV is given in figure 3 as a solid curve. One sees that the agreement for  $E > 60 \text{ MeV}$  is remarkably good for so few adjustable parameters.

Also plotted in figures 1 and 2 are values of  $V$ ,  $W_D$ , and  $W_V$  deduced from analyses of proton -  $^{208}\text{Pb}$  scattering using an average geometry for the potentials (see Table III of [6]). For  $W_V$  and  $W_D$ , only searches for which both  $W_V$  and  $W_D$  were free parameters are included.

Lane potentials can be determined from the neutron and proton potential depths shown above provided that the proton Coulomb energy  $\Delta_c$  is known (see, e.g., [5]). For  $V$ , as in [5], we define  $\Delta_c$  to be equal to the Coulomb displacement energy of the  $^{209}\text{Pb}$ - $^{209}\text{Bi}$  isobaric pair, 18.82 MeV. For  $W_V$ ,  $\Delta_c$  can be estimated by inspection of figure 2(a). We see here that the solid line (neutron data) and dashed line (proton data) essentially coincide. This result is consistent with the interpretation that for  $W_V$ ,  $\Delta_c$  as well as the volume imaginary symmetry potential  $W_{V1}$  are negligible. Since thresholds for nucleon-induced nuclear reactions are related to incident nucleon energies at infinity, the finding here that  $\Delta_c \approx 0$  is reasonable. The conclusion  $W_{V1} \approx 0$  is in accord with extensive global analyses performed at low energies [12] and high energies [10]. Since we are not aware of any compelling reasons for assigning different  $\Delta_c$  to the surface imaginary and volume imaginary potentials, we assume that  $\Delta_c \approx 0$  for the surface imaginary potential, also.

The validity of the Lane potentials thus determined was tested by comparing computed neutron total cross sections with experimental values for the spherical nuclei  $^{40}\text{Ca}$  and  $^{90}\text{Zr}$ . Initially the energy range 15 - 65 MeV was investigated. Computed  $\sigma_t$  over this energy range exhibited discrepancies at the minima near 20 MeV and 30 MeV for  $^{40}\text{Ca}$  and  $^{90}\text{Zr}$ , respectively, which indicated that the imaginary potential strength was too large at these energies. Calculations were then performed with the  $W_D$  for  $^{208}\text{Pb}$ . For both  $^{40}\text{Ca}$  and  $^{90}\text{Zr}$ , agreement between the calculated values and the experimental data was within the normalization uncertainty of the data, which is  $< 3\%$  [9].

Since we have found that for a wide range of  $A$ ,  $W_D$  and  $W_V$  can be represented by values deduced from  $n$ - $^{208}\text{Pb}$  scattering, only  $V$  must be modified to extend these results to higher energies. For the solid curves in figure 3,  $V$  at high energies was deduced for both  $^{40}\text{Ca}$  and  $^{90}\text{Zr}$  using a procedure identical to that for  $^{208}\text{Pb}$ :  $V(E)$  was converted from a linear function to a logarithmic function at 58 MeV. We point out that since  $V(E)$  is known in each case for  $E \leq 58$  MeV (it is the real Lane potential) and the transition energy is given, this procedure entails no free parameters. One observes that the agreement with the data is within experimental

uncertainties over a very wide energy range. Because we do not include in our analysis an imaginary spin orbit term (see, e.g., [10]) the good agreement above 200 MeV is unexpected. We point out, also, that the increase in the *calculated curves* for  $E \geq 290$  MeV is not caused by pion production. Our expression for  $W_v(E)$  does not take pion production explicitly into account. We find that for  $^{208}\text{Pb}$ ,  $\sigma_t$  increases for  $E > 290$  MeV even if each potential strength,  $V$ ,  $W_v$ , and  $V_s$ , is held fixed at its value at 290 MeV. This rise in  $\sigma_t$  could be associated with the spin orbit term of the phenomenological potential. Relative to the central potential, the spin orbit term increases in importance with increasing energy (see, e.g., [10]).

Our parameters provide a good fit to Pb  $\sigma(\theta)$  data at 155 MeV, which extend only to  $10^\circ$  [13]. Since these parameters predict  $\sigma_t$ , good agreement with  $\sigma(\theta)$  at forward angles is expected. However, because we do not include an imaginary spin orbit term in our model, predictions of analyzing powers at high energies would likely be qualitative at best.

To summarize, we have determined the symmetry dependence of the central part of the phenomenological optical model potential for neutron-nucleus scattering from about 15 to 65 MeV. In contrast to the case for incident protons, we find evidence that the symmetry dependence of the surface imaginary potential is negligible. When extended to higher energies, predictions of the model are in good agreement with measured neutron total cross sections for spherical nuclei over a wide range of  $A$  and incident energy with no adjustment of parameters.

A detailed version of the present study will be reported elsewhere.

## References

- [1] Haouat G *et al Report* CEA-N-2200 1981
- [2] Finlay R W *et al Phys. Rev. C* **30** 796 1984 and references therein
- [3] De Vito R P Ph.D. Thesis Michigan State University 1979
- [4] Hjort E L *et al Phys. Rev. C* **50** 275 1994
- [5] Schutt R L *et al Phys. Lett. B* **203** 22 1988
- [6] van Oers W T H *et al Phys. Rev. C* **10** 307 1974
- [7] Shamu R E and Young P G *J. Phys. G: Nucl. Part. Phys.* **19** L169 1993
- [8] Shamu R E, Schutt R L and Ferguson S M *Bull. Am. Phys. Soc.* **41** 1236 1996
- [9] Finlay R W *et al Phys. Rev. C* **47** 237 1993
- [10] Schwandt P *et al Phys. Rev. C* **26** 55 1982 and references therein
- [11] Shamu R E *et al J. Phys. G: Nucl. Part. Phys.* **17** 525 1991
- [12] Becchetti F D and Greenlees G W *Phys. Rev.* **182** 1190 1969
- [13] Harding R S *Phys. Rev.* **111** 1164 1958

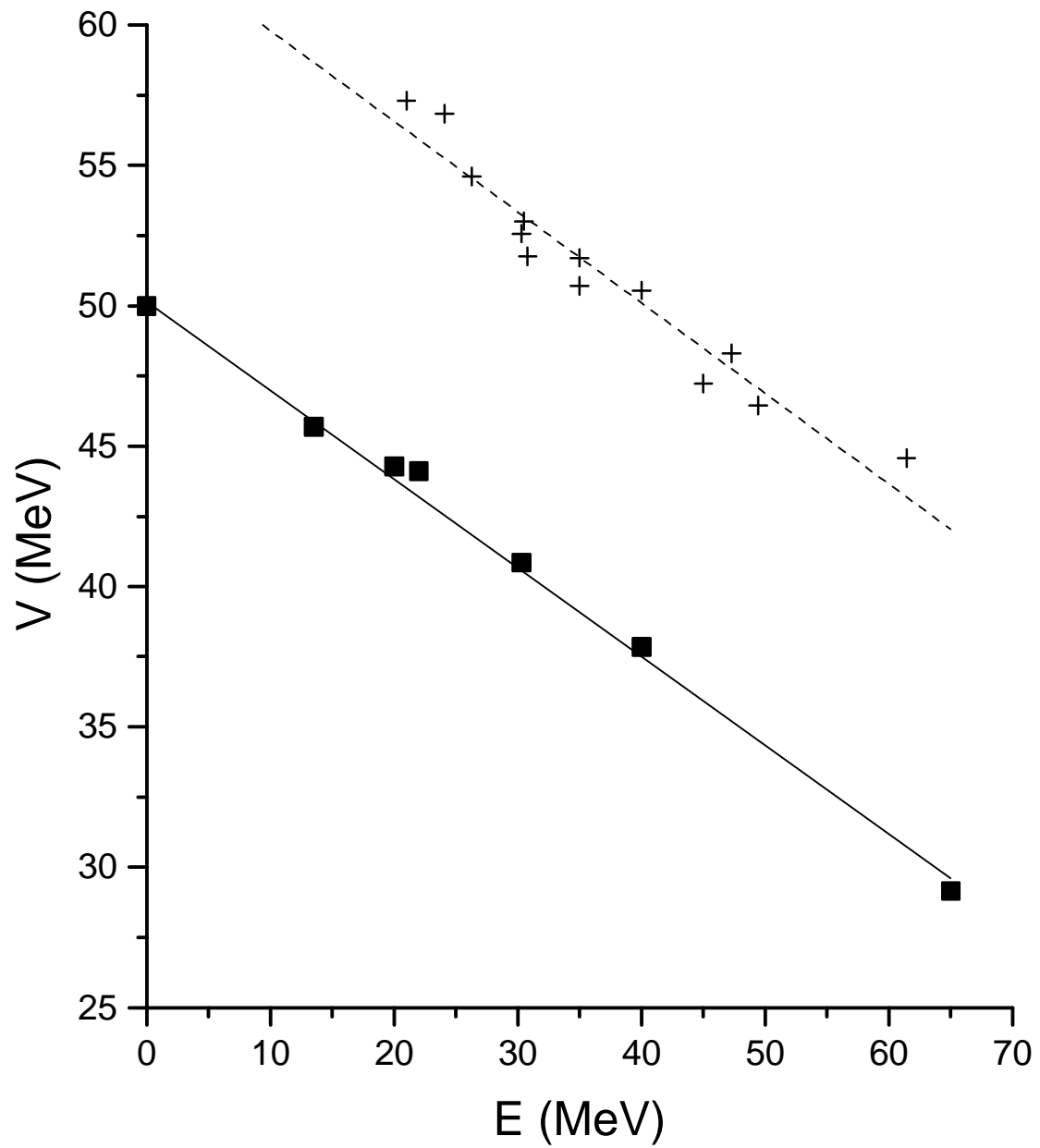


Figure 1. Strength of the real phenomenological optical potential for protons (pluses) and neutrons (solid squares) against incident nucleon energy for nucleons on  $^{208}\text{Pb}$ . Proton strengths are from [6]. The lines are least squares fits.

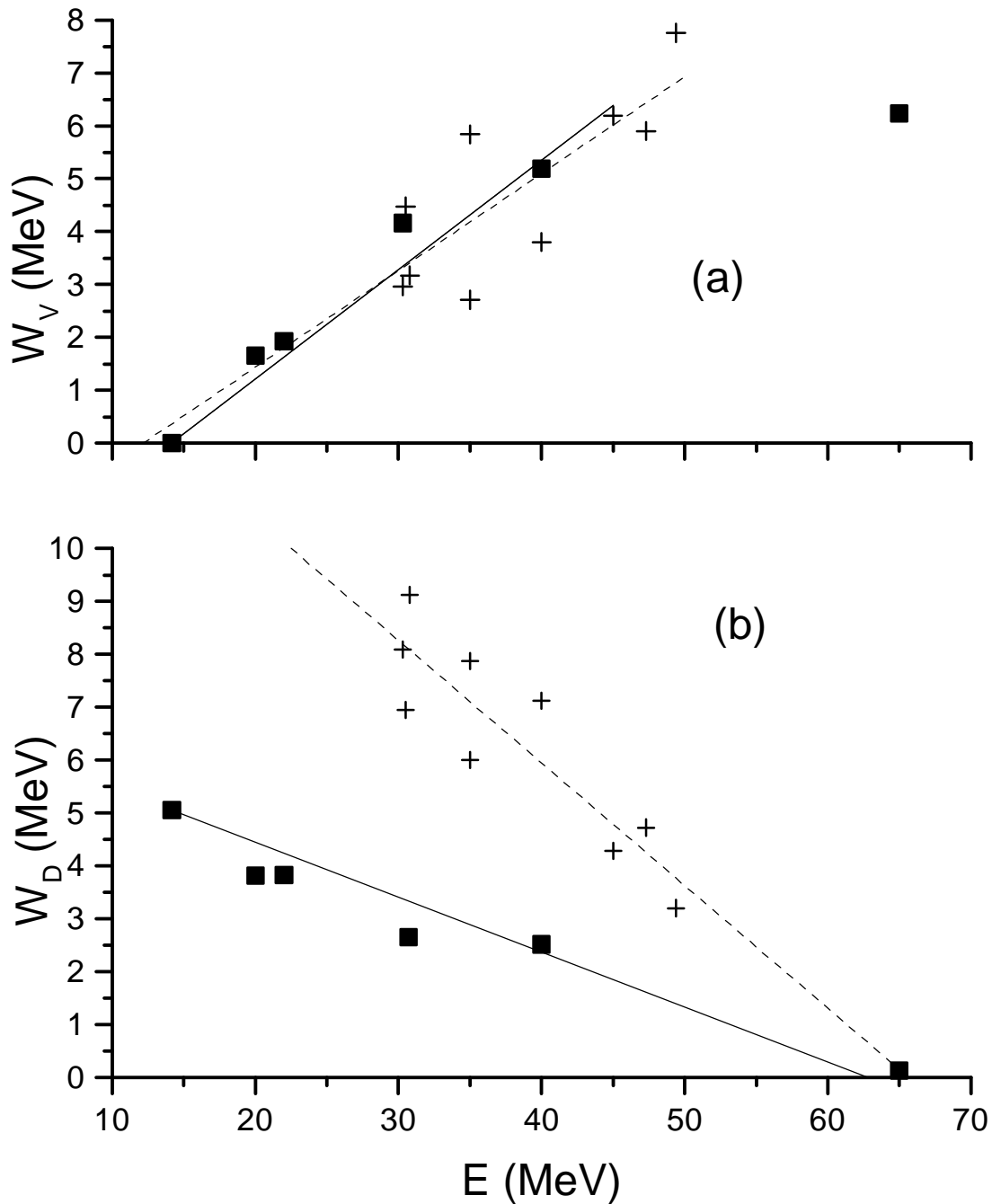


Figure 2. (a) Strength of the volume imaginary optical potential for protons (pluses) and neutrons (solid squares) against incident nucleon energy for nucleons on  $^{208}\text{Pb}$ . Proton strengths are from [6]. The dashed line is a least squares fit to proton values. The solid line is a fit to neutron values which is constrained to pass through the datum at 14 MeV. (b) Strength of the surface imaginary optical potential against incident nucleon energy for nucleons on  $^{208}\text{Pb}$ . See (a) for details.

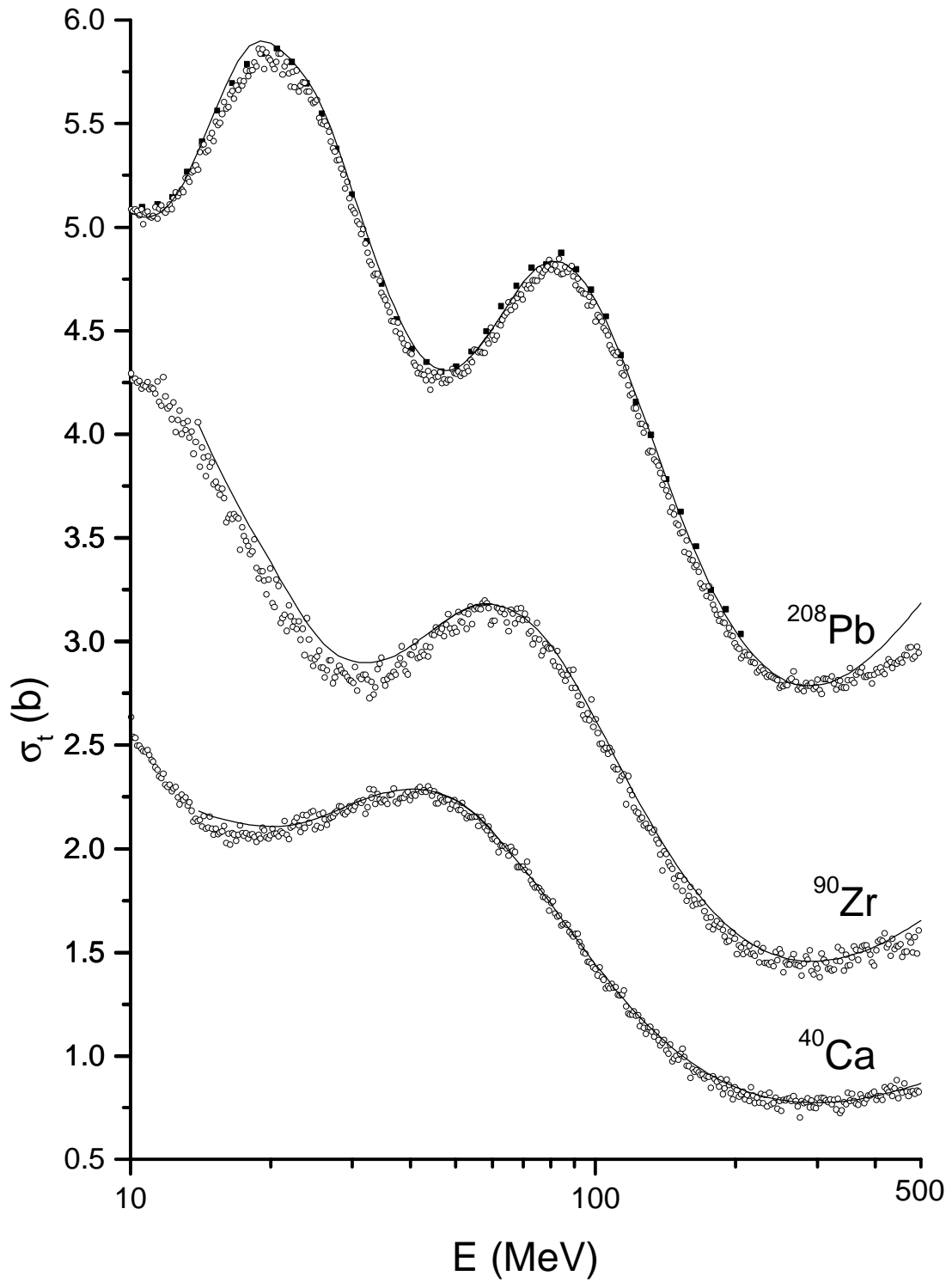


Figure 3. Total cross section versus energy for neutrons on  $^{40}\text{Ca}$ ,  $^{90}\text{Zr}$  and  $^{208}\text{Pb}$ . Data are from [5] (solid squares) and [9] (open circles). The curves represent computed cross sections. See text for details.